JOINT INSTITUTE FOR NUCLEAR RESEARCH

DZHELEPOV LABORATORY OF NUCLEAR PROBLEMS

WAVE 11 – 05 NOVEMBER TO 14 DECEMBER

RADIATION PROTECTION AND THE SAFETY OF RADIATION SOURCES

STUDENT: **R A THANUSH**

Institute of Chemical Technology, Mumbai, Indian Oil Campus,
Bhubaneswar, Odisha, India.

SUPERVISOR:: DR SAID ABOUELAZM

Dzhelepov Laboratory of Nuclear Problems

ABSTRACT

Radiation protection, as defined by the IEA, involves safeguarding people from the harmful effects of ionizing radiation and implementing measures to achieve this objective. Exposure can originate from external radiation sources or internal irradiation through the ingestion of radioactive contamination. Key principles of radiation protection include minimizing exposure duration, maximizing distance from the radiation source, and employing effective shielding to reduce dose levels. These fundamental strategies form the basis of ensuring safety in environments involving ionizing radiation.

Radiation detectors convert radiation interactions into measurable signals, providing critical data for ensuring safety and advancing technologies. The key principles behind radiation detection involve energy deposition, signal amplification, and data processing. Analyzing the detected radiation was the main part of this project. The tasks assigned by the professor were completed using various software including ROOT, Origin Analysis, Excel, and SRIM simulation, based on test data obtained in the laboratory. The final data was used to compare the technical data of the BGO and NaI detectors. Unknown sources are identified using the equation of the calibration line with known energy. The attenuation coefficients of aluminum and copper and the range of alpha particles in air are determined.

A hands-on experience in dealing with radiation data through the identification of unknown sources by using energy calibration curves, calculation of Resolution of different scintillation detectors, determination of alpha range in air using Pixel and Plastic detectors, determination of Attenuation coefficient for different materials, and the assessment of the ranges and energy of alpha particles using Monto Carlo simulation SIRM software were also undertaken.

CONTENT

INTRODUCTION

Radiation refers to the emission or transmission of energy in the form of waves or particles. It can be broadly categorized into non-ionizing radiation, such as radio waves and microwaves, and ionizing radiation, which has sufficient energy to remove tightly bound electrons from atoms, creating ions. Examples of ionizing radiation include alpha particles, beta particles, gamma rays, and X-rays.

Radiation Protection is the science and practice of safeguarding humans and the environment from the harmful effects of ionizing radiation while enabling its beneficial uses in medicine, industry, and research. Effective radiation protection involves controlling exposure to radiation sources, implementing safety protocols, and fostering a culture of awareness.

Radiation safety is guided by recommendations from authoritative bodies like the International Atomic Energy Agency (IAEA), the International Commission on Radiological Protection (ICRP), and the United Nations Scientific Committee on the Effects of Atomic Radiation (UNSCEAR). These organizations establish exposure limits, promote best practices, and develop protocols to ensure the safe use of radiation in medical, industrial, and environmental contexts, emphasizing global uniformity in safety standards.

Radiation protection is essential across various fields. In the medical field, it ensures the safety of patients and workers during diagnostic imaging, radiotherapy, and nuclear medicine procedures. In the nuclear industry, it mitigates risks in power plants and research facilities. Environmental monitoring focuses on identifying and managing natural and human-made radiation sources. These applications highlight the balance between utilizing the benefits of radiation and safeguarding against its risks. By understanding and applying these principles, we can effectively manage the risks of ionizing radiation, enabling its safe and beneficial use in numerous domains.

The main objective of this project is to establish a solid foundation for radiation protection and radiation sources. Additionally, provides the necessary practical skills and basic tools for those interested in working in the field of radiation protection and the safe use of radiation sources through a series of laboratory works.

Radiation Dose

The term radiation dose refers to the amount of radiation absorbed by a substance or organism. It encompasses three critical measures: absorbed dose, which is the energy deposited by ionizing radiation per unit mass of tissue, measured in grays (Gy); equivalent dose, which adjusts for the type of radiation and its biological effects, measured in sieverts (Sv); and effective dose, which considers the varying sensitivities of different tissues and organs, offering an overall risk estimate. These measures help quantify exposure and enable effective monitoring and management of radiation risks.

The effects of ionizing radiation are quantified using standardized units. The gray (Gy) measures the absorbed dose, indicating the energy absorbed per kilogram of tissue. However, to account for the biological effects of different radiation types, the sievert (Sv) is used, adjusting for effectiveness in causing biological damage. These units provide a consistent framework for assessing exposure and implementing protective measures across diverse applications.

Radiation protection

Radiation protection relies on three core principles to minimize harm: time, distance, and shielding. Reducing the time spent near a radiation source lowers the absorbed dose proportionally. Maximizing distance from the source decreases dose intensity significantly due to the inverse-square law. Using appropriate shielding materials, such as lead, concrete, or water, further blocks or reduces radiation intensity. These strategies are integral to safeguarding individuals in environments where ionizing radiation is present.

Radio Active Decay

Radioactive decay (also known as nuclear decay, radioactivity, radioactive disintegration, or nuclear disintegration) is the process by which an unstable atomic nucleus loses energy by radiation. A material containing unstable nuclei is considered radioactive. Three of the most common types of decay are alpha decay (α-decay), beta decay (β-decay), and gamma decay (γ-decay), all of which involve emitting one or more particles. The weak force is the mechanism that is responsible for beta decay, while the other two are governed by electromagnetism and nuclear force. A fourth type of common decay is electron capture, in which an unstable nucleus captures an inner electron from one of the electron shells. The loss of that electron from the shell results in a cascade of electrons dropping down to that lower shell resulting in the emission of discrete X-rays from the transitions. A common example is iodine-125 commonly used in medical settings.

Half-Life

Half-life (symbol t½) is the time required for a quantity (of substance) to reduce to half of its initial value. The term is commonly used in nuclear physics to describe how quickly unstable atoms undergo radioactive decay or how long stable atoms survive. The term is also used more generally to characterize any type of exponential (or, rarely, non-exponential) decay. For example, the medical sciences refer to the biological half-life of drugs and other chemicals in the human body. The converse of half-life (in exponential growth) is doubling time. Half-life is the length of time it takes for half of the radioactive atoms of a specific radionuclide to decay. A good rule of thumb is that, after seven half-lives, you will have less than one percent of the original amount of radiation.

JINR- JOINT INSTITUTE OF NUCLEAR RESEARCH

The Joint Institute for Nuclear Research (JINR), in Dubna, Moscow Oblast (110 km north of Moscow), Russia, is an international research center for nuclear sciences, with 1200 researchers including 1000 Ph.Ds from eighteen countries, like Armenia, Azerbaijan, Belarus, Kazakhstan and Ukraine, members of the institution. The institute has seven laboratories, each with its specialization: theoretical physics, high energy physics (particle physics), heavy ion physics, condensed matter physics, nuclear reactions, neutron physics, and information technology. The institute has a division to study radiation and radiobiological research and other ad hoc experimental physics experiments. Principal research instruments include a nuclotron superconductive particle accelerator (particle energy: 7 GeV), three isochronic cyclotrons (120, 145, 650 MeV), a phasotron (680 MeV) and a synchrophasotron (4 GeV). The site has a neutron fast-pulse reactor (1500 MW pulse) with nineteen associated instruments receiving neutron beams.

Scintilllator Detector

A scintillation counter is an instrument for detecting and measuring ionizing radiation by using the excitation effect of incident radiation on a scintillating material and detecting the resultant light pulses. It consists of a scintillator which generates photons in response to incident radiation, a sensitive photodetector (usually a photomultiplier tube (PMT), a charge-coupled device (CCD) camera, or a photodiode), which converts the light to an electrical signal and electronics to process this signal. Scintillation counters are widely used in radiation protection, assay of radioactive materials, and physics research because they can be made inexpensively yet with good quantum efficiency, and can measure both the intensity and the energy of incident radiation.

A scintillation counter is used to detect gamma rays and the presence of a particle. It can also measure the radiation in the scintillating medium, the energy loss, or the energy gain. The medium can either be gaseous, liquid, or solid. The scintillator counter is generally comprised of transparent crystalline material such as glasses, liquids, or plastics. One sector of the scintillators is placed (optical contact) with the pin code.

A charged particle loses energy when passing through the scintillator thus leaving a trail of excited molecules and atoms. A rapid interatomic transfer of electronic excitation energy follows, which leads to the burst of scintillator material luminescence characteristics. The scintillation response is when a particle stops leading to the light output. The energy loss of a particle is measured when a particle passes completely through a scintillator.

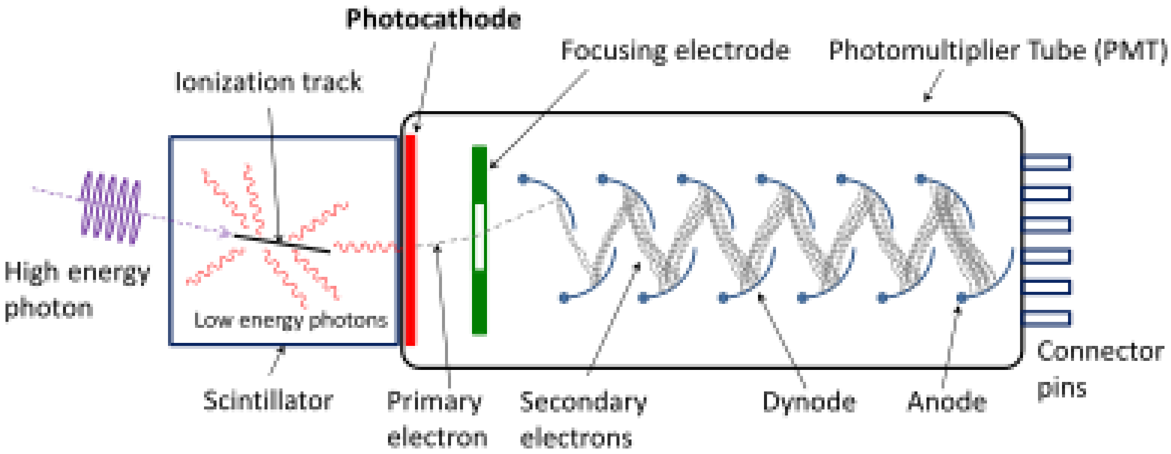

Pixel detector

The pixel detector, though only about the size of a small suitcase, contains 124 million pixels, allowing it to track the paths of particles emerging from the collision with extreme accuracy. It is also the closest detector to the beam pipe, with cylindrical layers roughly at 3cm, 7cm, 11cm, and 16cm and disks at either end and so will be vital in reconstructing the tracks of very short-lived particles. Each of the four layers is composed of individual silicon modules, split into little silicon sensors, like tiny kitchen tiles: the pixels. Each of these silicon pixels is 100µm by 150µm, about two hairs widths. When a charged particle passes through a pixel, it gives enough energy to eject the electrons from silicon atoms. A voltage applied to the sensor allows the collecting of these charges as a small electric signal, which is amplified by an electronic readout chip (for a total of 16 chips per module).

Pixel detectors for precise particle tracking in high-energy physics have been developed to a level of maturity during the past decade. Three of the LHC detectors will use vertex detectors close to the interaction point based on the hybrid pixel technology which can be considered the 'state of the art‘ in this field of instrumentation. A development period of almost 10 years has resulted in pixel detector modules that can stand the extreme rate and timing requirements as well as the very harsh radiation environment at the LHC without severe compromises in performance. From these developments, several different applications have spun off, most notably for biomedical imaging. Beyond hybrid pixels, several monolithic or semi-monolithic developments, which do not require complicated hybridization but come as single sensor/IC entities, have appeared and are currently developed to reader maturity. Most advanced in terms of maturity are the so-called CMOS active pixels and DEPFET pixels.

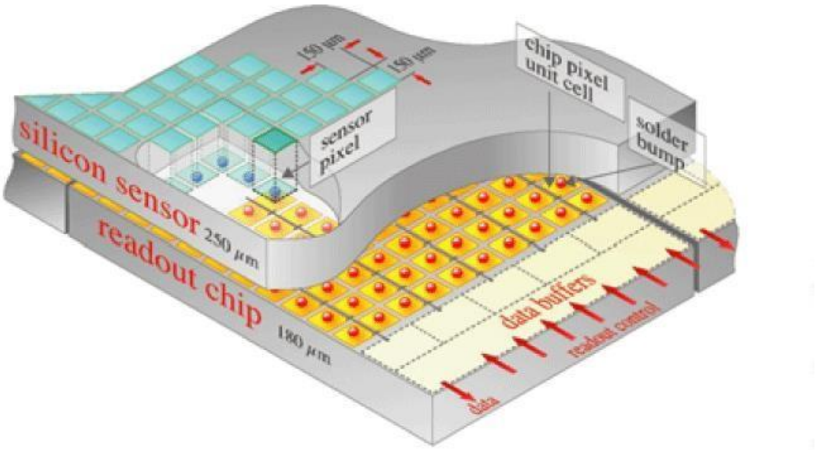

BGO Detector

Bismuth germanium oxide or bismuth germanate is an inorganic chemical compound of bismuth, germanium, and oxygen. Most commonly the term refers to the compound with the chemical formula $Bi_4Ge_3O_{12}$ (BGO), with the cubic evlitine crystal structure, used as a scintillator. (The term may also refer to a different compound with the formula $Bi_{12}GeO_{20}$, an electro-optical material with a selenite structure, and $Bi_2Ge_3O_9$.) BGO stands for bismuth germanate, which is a scintillation material used in detectors for detecting and measuring high-energy gamma rays and X-rays. BGO detectors consist of a crystal of bismuth germanate, which is a dense and high atomic number material that is capable of absorbing high-energy photons and emitting scintillation light. They have several advantages over other scintillation materials, including high density, high atomic number, and high light yield, which makes them well-suited for detecting high-energy photons. They also have a relatively fast response time and good energy resolution, which makes them useful for a wide range of applications, including in nuclear medicine, high-energy physics, and homeland security.

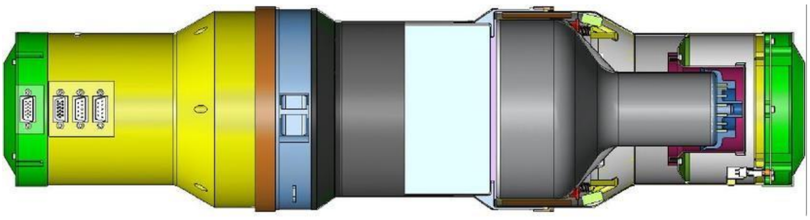

NAI Detector

NAI stands for NaI(Tl)--based scintillation detector, which is a type of radiation detector that uses a crystal of sodium iodide doped with thallium (NaI(Tl)) as the scintillator material. The thallium-activated sodium iodide detector, or NaI(Tl) detector, responds to the gamma-ray by producing a small flash of light, or a scintillation. The scintillation occurs when scintillator electrons, excited by the energy of the photon, return to their ground state. NAL detectors are commonly used in nuclear medicine, environmental monitoring, and radiation safety applications for detecting and measuring gamma rays and X-rays. They have several advantages over other types of scintillation detectors, including a high light output, good energy resolution, and relatively low cost. However, NAL detectors also have some disadvantages, such as a relatively slow response time and sensitivity to temperature and humidity variations.

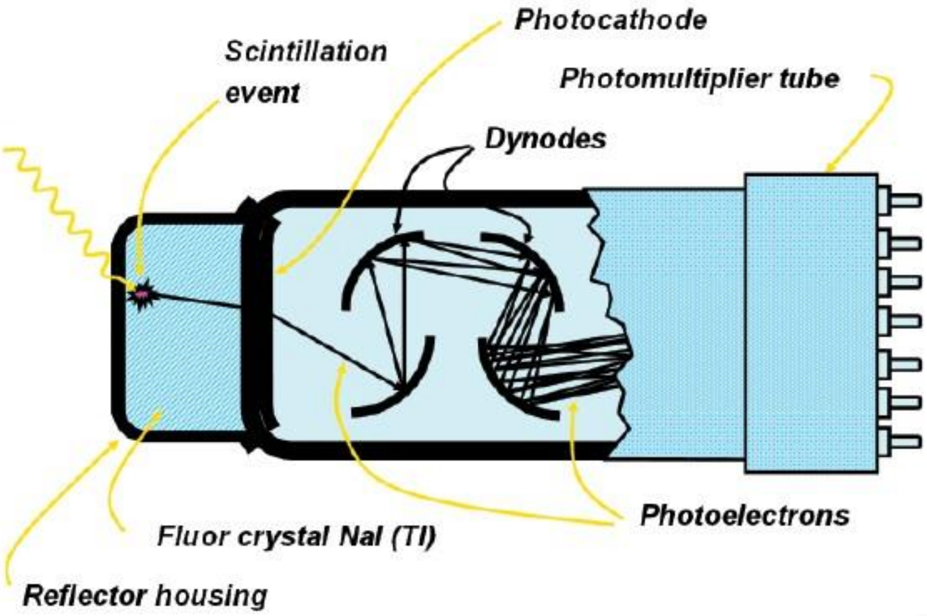

Task 1.1: Relation between the Resolution and Applied Voltage for BGO detectors

The energy resolution of a detector refers to its ability to separate signals or peaks and accurately determine the energy of the incoming radiation. The better the energy resolution, the finer it can distinguish two adjacent energy peaks, allowing the identification of different decays or radionuclides in the spectrum. The resolution is calculated from the peak at full-width half maximum (FWHM) divided by the location of the peak centroid, $H0$:

$Resolution=(\sigma/Mean)*2.35$

mean	Sigma	Voltage (v)	Resolution(%)
1.3257	0.195395	1300	35%
1.91095	0.2786632	1400	34%
2.99922	0.39737	1500	31%
4.38902	0.502282	1600	27%
6.10903	0.746833	1700	29%
10.6832	1.25572	1900	28%
13.6672	1.49012	2000	26%

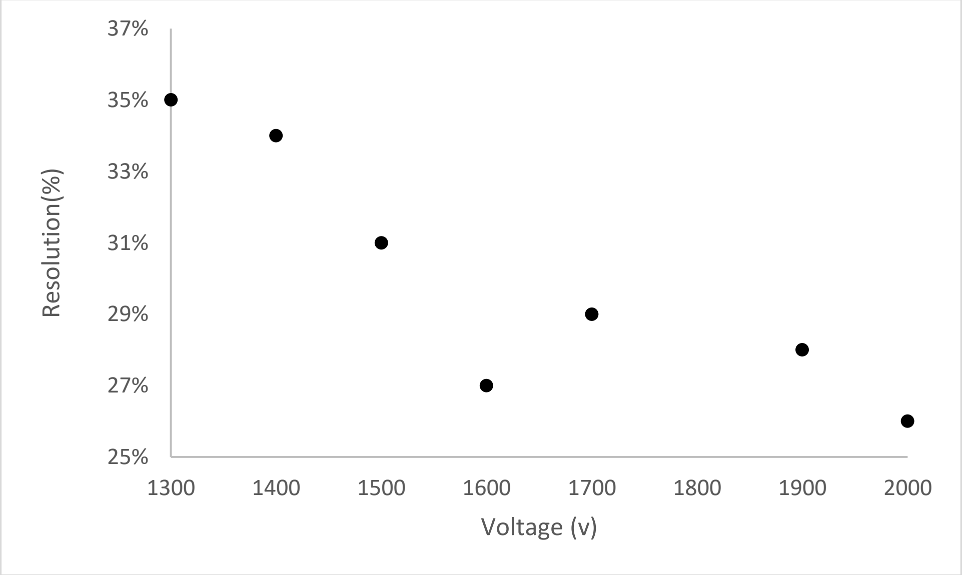

Task 1.2: Calibration Of BGO Detector

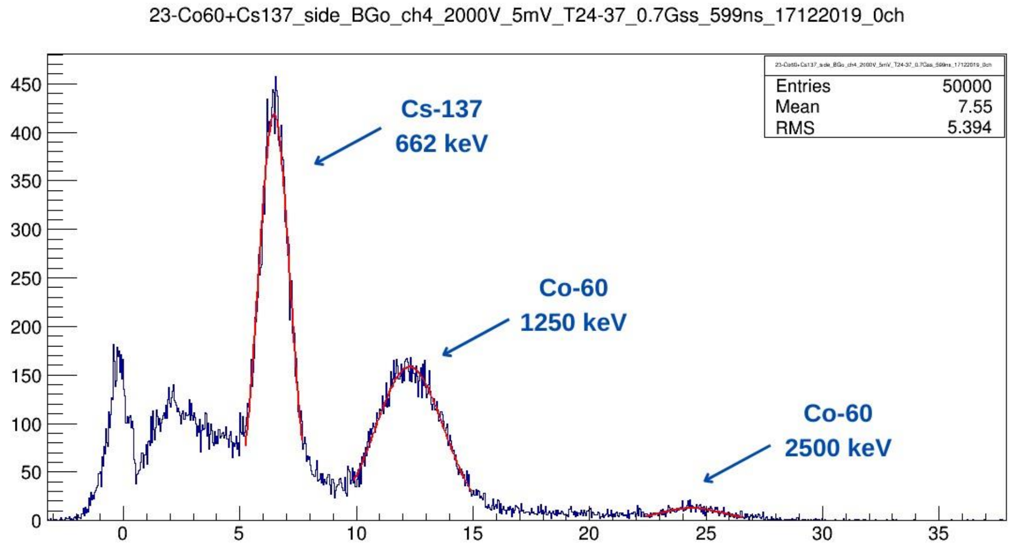

Isotope	Channel	Energy(keV)
Cs-137	6.475	662
Co-60	12.279	1250
	24.379	2500

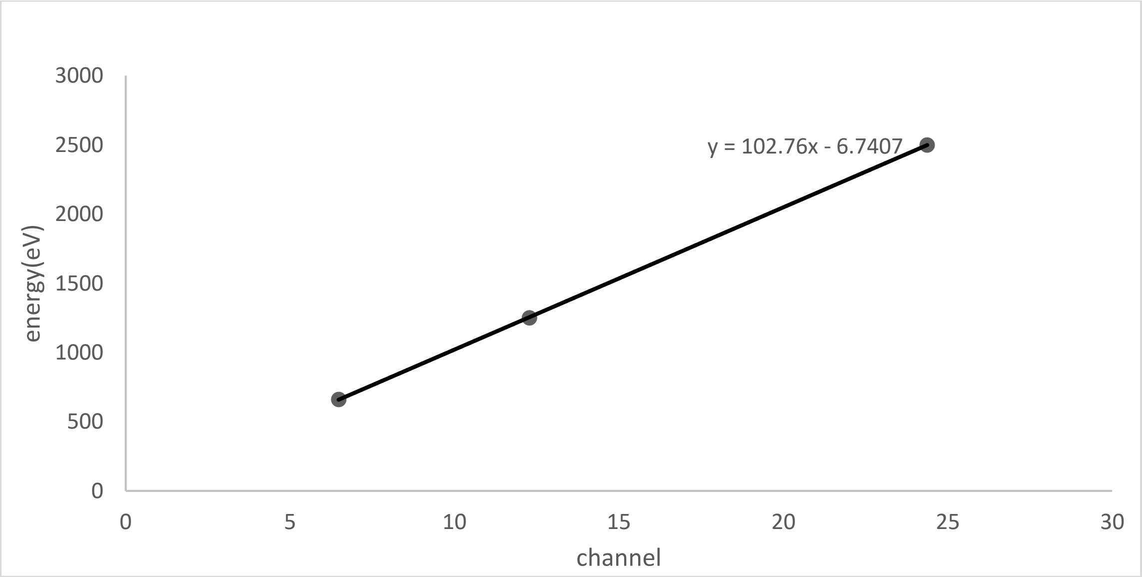

The equation of the energy calibration line for the BGO detector is:

$\boldsymbol{y=102.7571x-6.74066}$

Where: x = channel number (mean), y = energy of the peaks (in keV)

Task 1.3: Identification Of Unknown Sources

For the identification of the energy spectrum and its unknown sources, the following steps can be applied:

i. Using the ROOT software, a Gauss function is fitted into the spectrum of the unknown energy, and the channel number (mean) is obtained.

ii. From the equation of the calibration line of the BGO detector, the channel number can be converted to energy.

iii. The unknown source of the calculated energy can be determined using the Nuclide Datasheet.

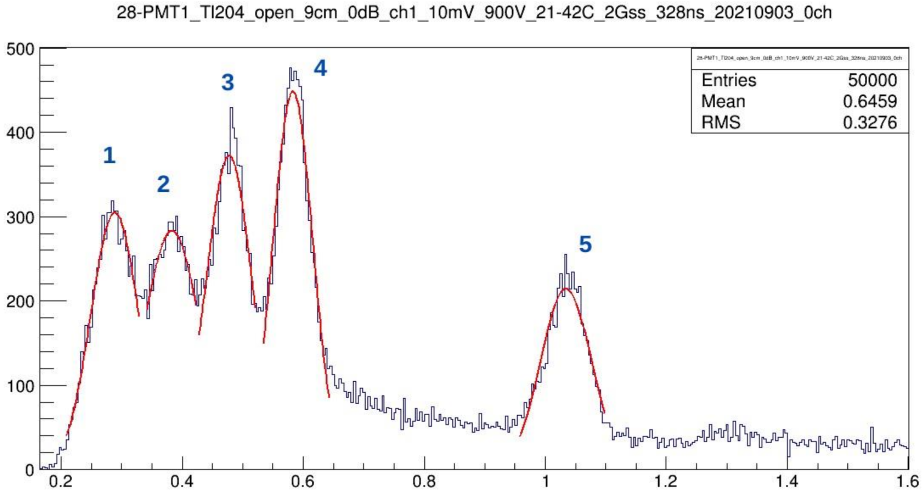

Peak	Channel	Energy (keV)	Energy (MeV)	Peak ID
1	0.289	22.956	0.022956	**Sm-151**
2	0.383	32.615	0.032615	**Mg-28**
3	0.478	42.377	0.042377	
4	0.583	53.167	0.053167	**Rh-104m**
5	1.034	99.510	0.099510	**Au-145**

Task 2.1: Relation between the Resolution and Applied Voltage for NAI detectors

The energy resolution of a detector refers to its ability to separate signals or peaks and accurately determine the energy of the incoming radiation. The better the energy resolution, the finer it can distinguish two adjacent energy peaks, allowing the identification of different decays or radionuclides in the spectrum. The resolution is calculated from the peak at full-width half maximum (FWHM) divided by the location of the peak centroid, $H0$:

$Resolution=(\sigma/Mean)*2.35$

mean	**Sigma**	**Applied Voltage (V)**	**Resolution (%)**
23.67	0.635	900	6.304
40.655	0.966	1000	5.584
65.792	1.514	1100	5.408
98.707	2.032	1200	4.838
137.35	2.616	1300	4.476

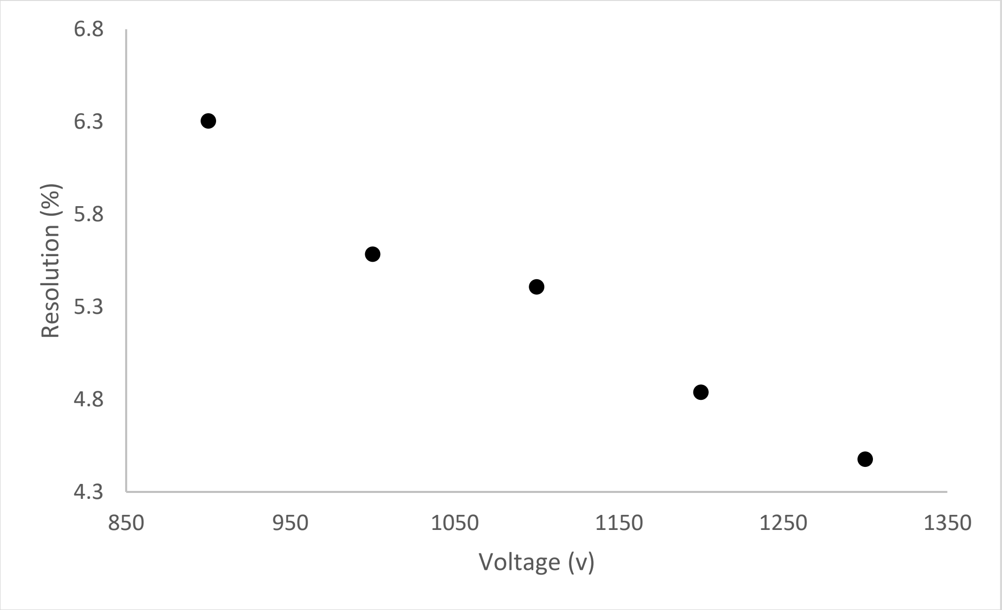

Task 2.2: Energy Calibration of NaI detectors at 800V

A NaI detector has more light output, so its resolution is twice as good as a BGO detector. It can separate the two peaks of Co-60 with energies of 1170 keV and 1330 keV, respectively. This is the reason that four peaks are visible instead of three, in the energy spectrum below.

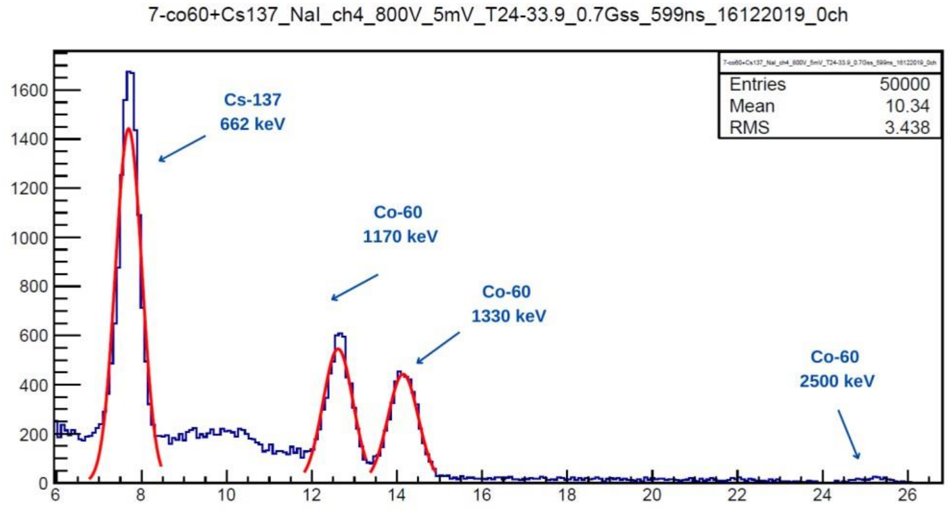

Isotope	Channel	Energy (keV)
Cs-137	7.696	**662**
Co-60	12.624	1170
Co-60	14.145	1330
C0-60	25.199	2500

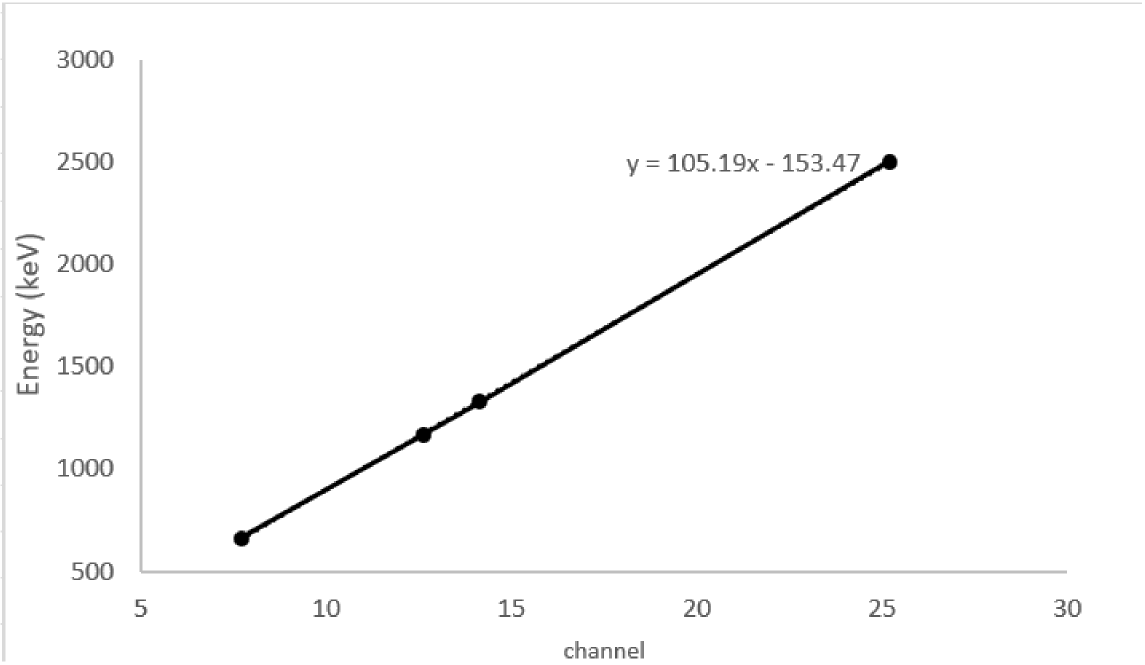

y=105.18685x−153.46699

Task 2.3: Identification of Unknown Sources

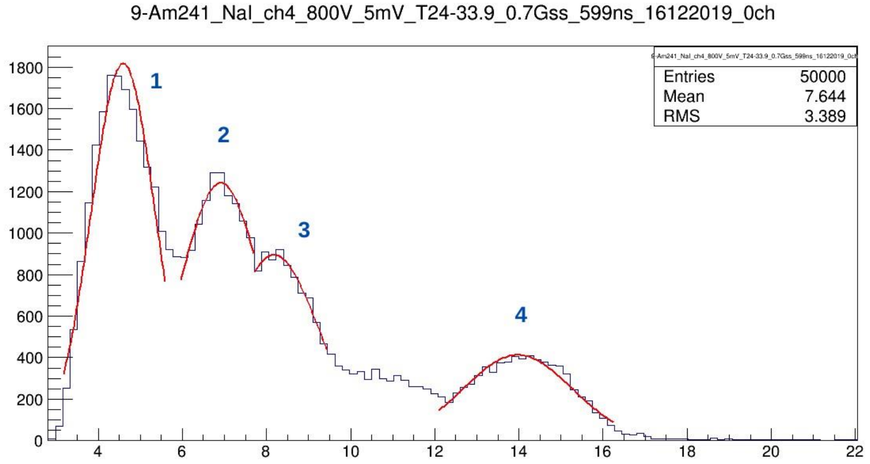

Peak	Channel	Energy (MeV)	Peak ID
1	4.593	329.656	Ir-194
2	6.915	573.9	Bi-207
3	8.178	706.751	Tc-129m
4	13.973	1316.309	Ca-47

Sample Calculation (Peak 1):

Equation of the calibration line: $\mathbf{y=105.18685x-153.46699;\ x=4.593.}$

Substitute the value of x: $y=105.18685*4.593-153.46699$

$y=329.656$ keV

Task 3: Resolution Of Semiconductor Cd-Te 1,2,3

Task 3.1 Resolution of cadmium telluride detector using Am-241

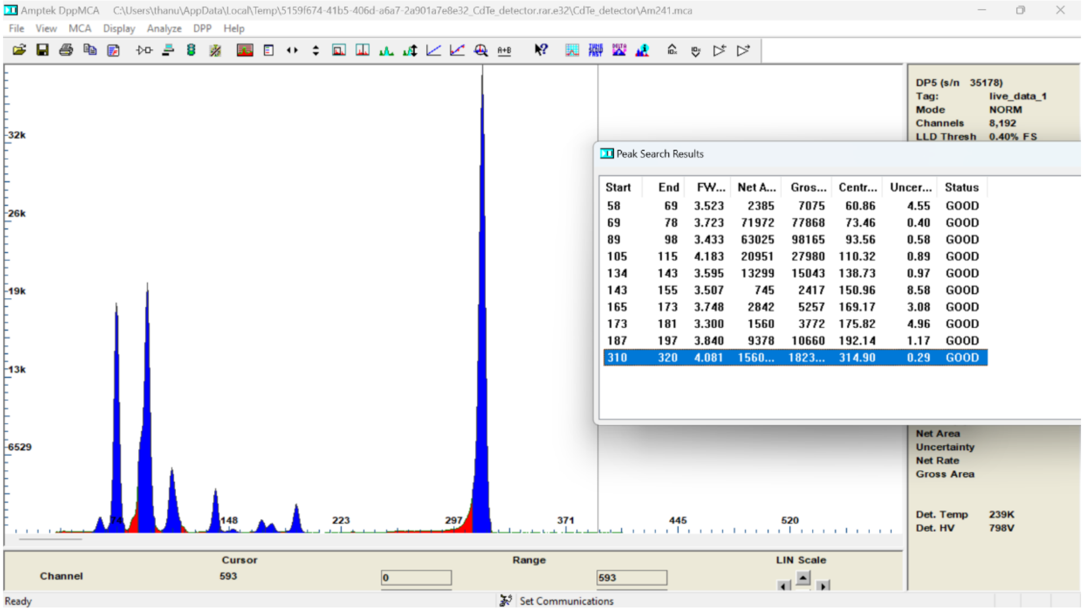

DP5 (s/n 35178)
Tag: live_data_1
Mode NORM
Channels 8,192
LLD Thresh 0.40% FS
Det. Temp 239K
Det. HV 798V
Channel 593
Range 0 593

Start	End	FW...	Net A...	Gros...	Centr...	Uncer...	Status
58	69	3.523	2385	7075	60.86	4.55	GOOD
69	78	3.723	71972	77868	73.46	0.40	GOOD
89	98	3.433	63025	98165	93.56	0.58	GOOD
105	115	4.183	20951	27980	110.32	0.89	GOOD
134	143	3.595	13299	15043	138.73	0.97	GOOD
143	155	3.507	745	2417	150.96	8.58	GOOD
165	173	3.748	2842	5257	169.17	3.08	GOOD
173	181	3.300	1560	3772	175.82	4.96	GOOD
187	197	3.840	9378	10660	192.14	1.17	GOOD
310	320	4.081	1560...	1823...	314.90	0.29	GOOD

Resolution =(FWHM/Centroid)*100

FWHM = 4.081
MEAN= 314.90

Resolution = 1.29

Task 3.2 Resolution of cadmium telluride detector using Am-243

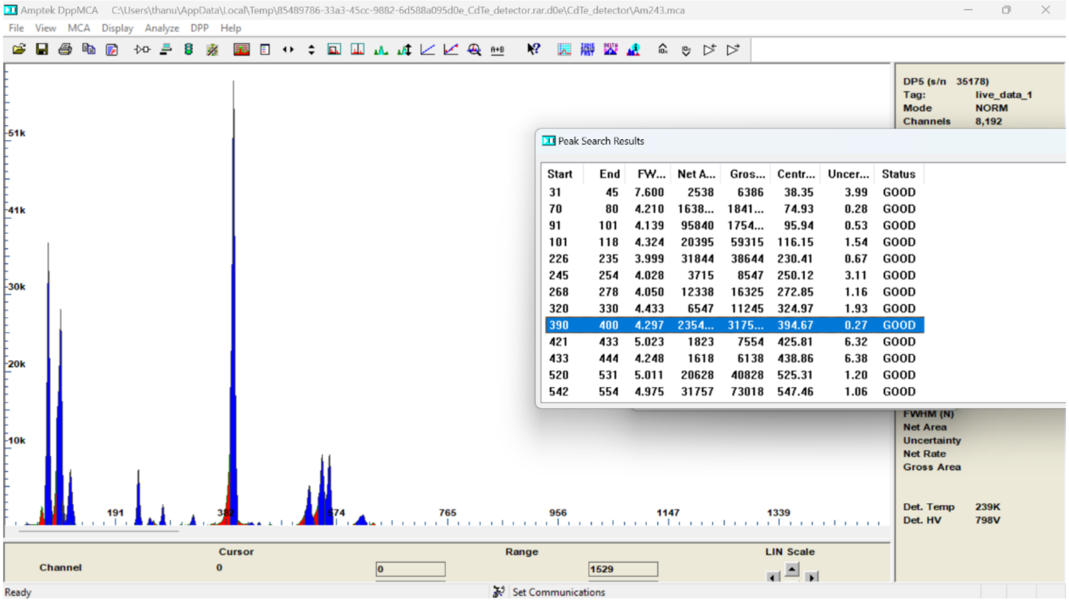

DP5 (s/n 35178)
Tag: live_data_1
Mode NORM
Channels 8,192
Det. Temp 239K
Det. HV 798V
Channel 0
Range 0 1529

Start	End	FW...	Net A...	Gros...	Centr...	Uncer...	Status
31	45	7.600	2538	6386	38.35	3.99	GOOD
70	80	4.210	1638...	1841...	74.93	0.28	GOOD
91	101	4.139	95840	1754...	95.94	0.53	GOOD
101	118	4.324	20395	59315	116.15	1.54	GOOD
226	235	3.999	31844	38644	230.41	0.67	GOOD
245	254	4.028	3715	8547	250.12	3.11	GOOD
268	278	4.050	12338	16325	272.85	1.16	GOOD
320	330	4.433	6547	11245	324.97	1.93	GOOD
390	400	4.297	2354...	3175...	394.67	0.27	GOOD
421	433	5.023	1823	7554	425.81	6.32	GOOD
433	444	4.248	1618	6138	438.86	6.38	GOOD
520	531	5.011	20628	40828	525.31	1.20	GOOD
542	554	4.975	31757	73018	547.46	1.06	GOOD

Resolution =(FWHM/Centroid)*100

FWHM = 4.297

MEAN= 394.67

Resolution =1.088

Task 3.3 Resolution of cadmium telluride detector using Co- 57

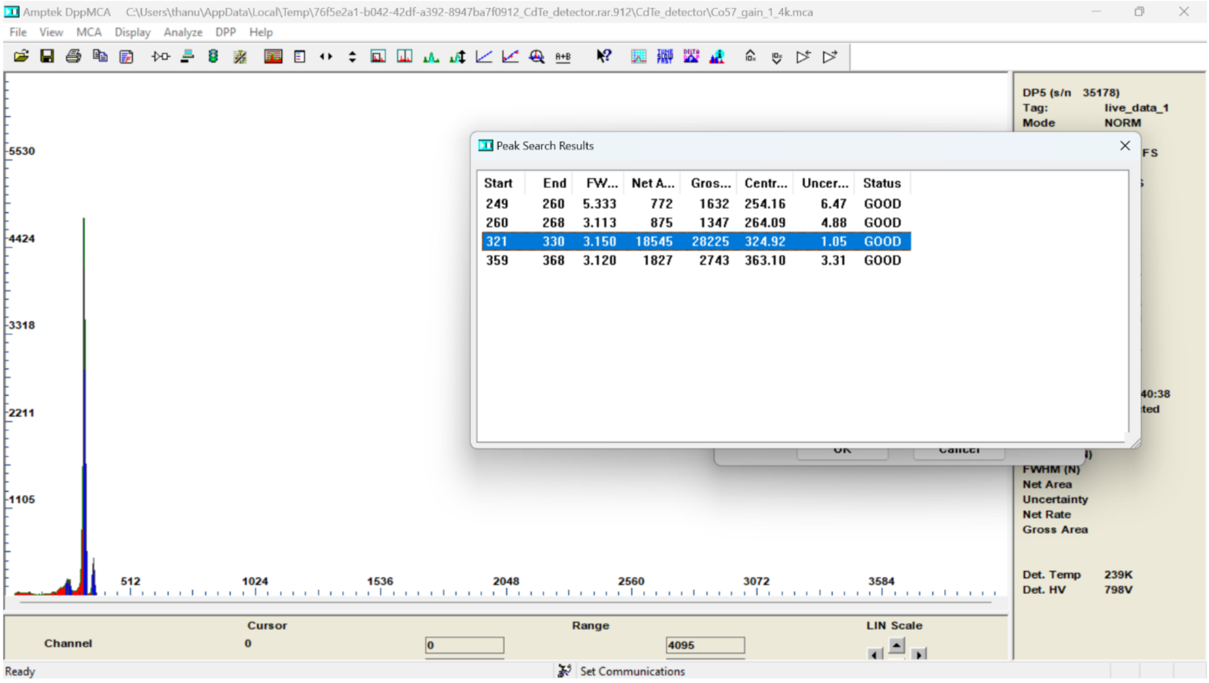

Peak Search Results

Start	End	FW...	Net A...	Gros...	Centr...	Uncer...	Status
249	260	5.333	772	1632	254.16	6.47	GOOD
260	268	3.113	875	1347	264.09	4.88	GOOD
321	330	3.150	18545	28225	324.92	1.05	GOOD
359	368	3.120	1827	2743	363.10	3.31	GOOD

DP5 (s/n 35178)
Tag: live_data_1
Mode NORM
Det. Temp 239K
Det. HV 798V

Channel
Cursor 0
Range 0 4095
LIN Scale

Resolution =(FWHM/Centroid)*100

FWHM = 3.150

MEAN= 324.92

Resolution =0.96

Task 3.4 Resolution of cadmium telluride detector using Cs- 137

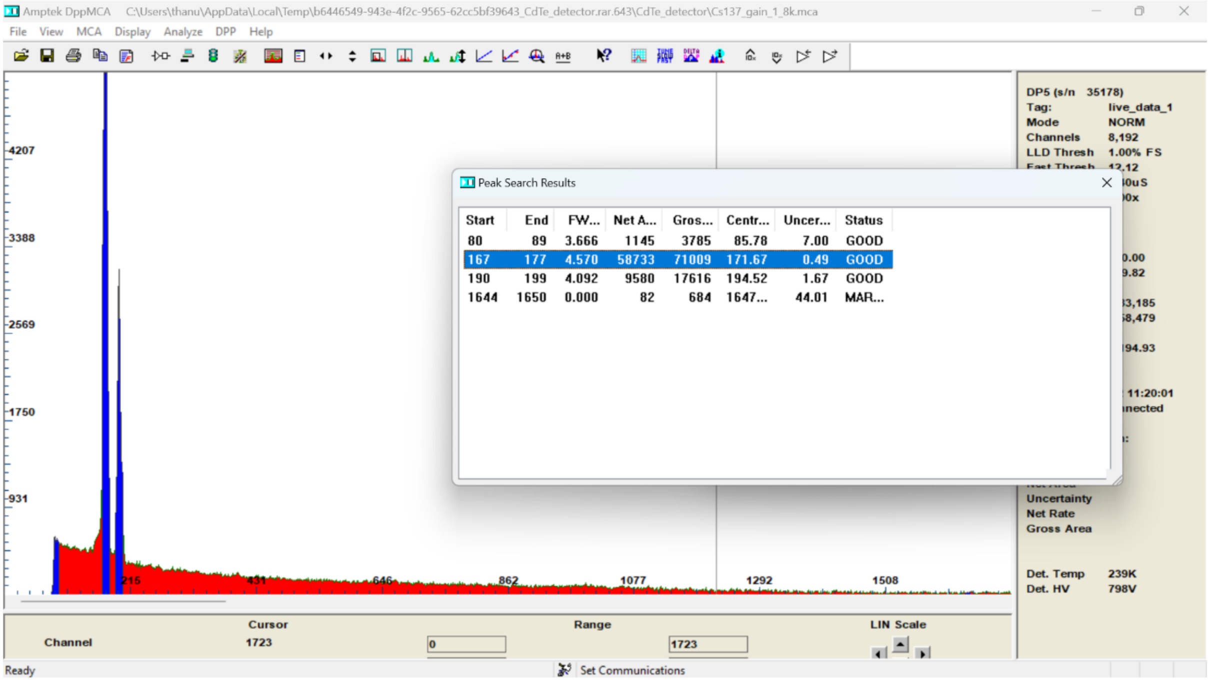

Amptek DppMCA   C:\Users\thanu\AppData\Local\Temp\b6446549-943e-4f2c-9565-62cc5bf39643_CdTe_detector.rar.643\CdTe_detector\Cs137_gain_1_8k.mca

Peak Search Results

```
Start   End   FW...  Net A...  Gros...  Centr...  Uncer...  Status
80       89   3.666     1145     3785     85.78      7.00   GOOD
167     177   4.570    58733    71009    171.67      0.49   GOOD
190     199   4.092     9580    17616    194.52      1.67   GOOD
1644   1650   0.000       82      684   1647...     44.01   MAR...
```

DP5 (s/n 35178)
Tag: live_data_1
Mode NORM
Channels 8,192
LLD Thresh 1.00% FS
Det. Temp 239K
Det. HV 798V

Resolution =(FWHM/Centroid)*100

FWHM = 4.570

MEAN= 171.67

Resolution =2.43

Task 3.5: Calibration of Cadmium telluride detector

Channel no.	Energy (eV)	Material
315	39181	Am241
395	61394	Am 243
172	13795	Cs137

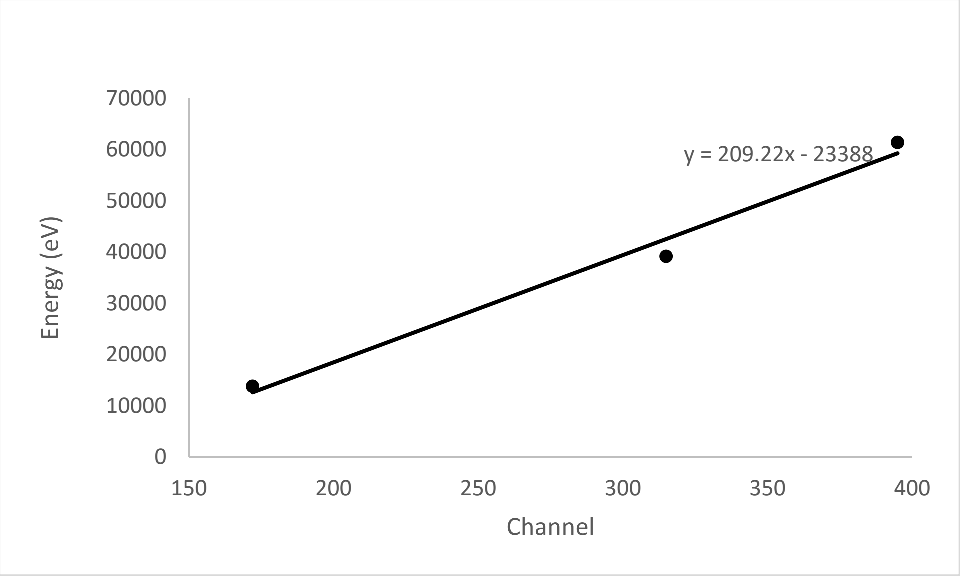

y = 209.22x - 23388

Task 4: Determination of the attenuation coefficient

Every material has its unique attenuation coefficient. Linear attenuation coefficient (μ) is a constant that describes the fraction of attenuated (absorbed or scattered) incident photons in a beam per unit thickness of a material. This covers all possible interactions such as coherent scattering, Compton scattering, and photoelectric effect. Linear attenuation coefficient can be calculated from the following formula: $I=I_0e^{-\mu x}$ Where:

x = absorber thickness,

I = intensity transmitted through an absorber of thickness x, I_0 = intensity at zero absorber thickness, μ = linear attenuation coefficient.

Linear attenuation coefficient has two main features: increases as the atomic number and physical density of the absorbing material increases, and it decreases with increasing photon energy (except at K-edges). Its variant is the mass attenuation coefficient, which is defined as a normalization of the linear attenuation coefficient per unit density of a material, resulting in a value that is constant for a given element or compound.

Experimental Equipment:

- • Detector: BGO detector
- • Voltage: 2000V
- • Radioactive source: Cs-137, E_{Cs}=662 keV
- • Attenuation material: Aluminum and Copper

4.1 Attenuation coefficient of Aluminum (Al)

Thickness (cm)	**I/I0**
0	1
0.15	0.75573
0.3	0.71623
0.45	0.70569
0.75	0.68596
0.9	0.67155
1.08	0.66103
1.26	0.63939

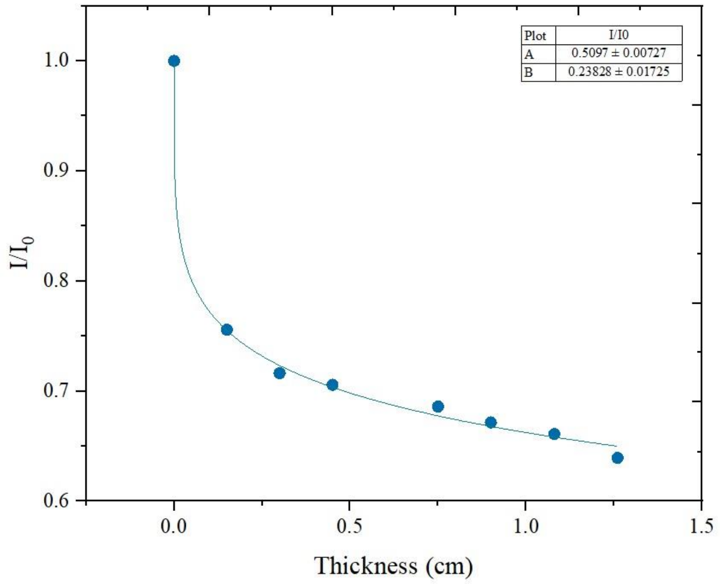

From the non-linear fitting curve in Origin Analysis, the obtained linear attenuation coefficient of aluminum (Al) is ***0.23828 ± 0.01725*** cm^{-1}.

4.2. Attenuation coefficient of Copper (Cu)

Thickness(cm)	I/I0
0	1
0.2	0.7393
0.25	0.7357
0.4	0.68065
0.8	0.58611
1	0.53827
1.2	0.48042

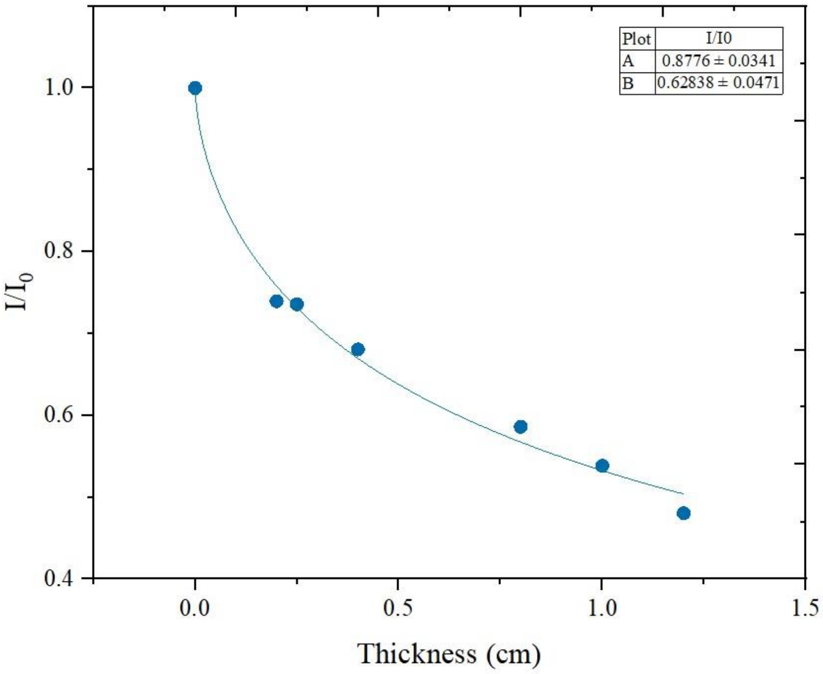

From the non-linear fitting curve in Origin Analysis, the obtained linear attenuation coefficient of copper (Cu) is ***0.62838 ± 0.0471 cm^{-1}***.

Task 5: Range of Alpha Particles in Air

Range is characterized as the path length that a particle travels from its source through the matter before it is stopped. It is influenced by the type of particle, its original kinetic energy, and the medium through which it travels. The range is especially important for charged particles, like electrons and alpha particles. Alpha particles particularly travel in almost straight lines because they are thousands of times heavier than atomic electrons, to which they lose energy slowly. Their range is usually measured in a straight line from the source to the point where ionization stops.

In this experiment, a plastic detector is used instead of a BGO detector. This is because the BGO detector has a thin aluminum foil layer and shielding can occur, leading to energy loss and inaccurate measurements.

Experimental Equipment:

- Radioactive Source: Pu-239
- Energy of He: 5.5 MeV
- Detector: Plastic Detector
- Voltage: 2000V

Distance (cm)	Counts/sec
0	440
0.5	390
1	360
1.5	340
2	320
2.5	300
3	280
3.5	260
3.8	260
4	260

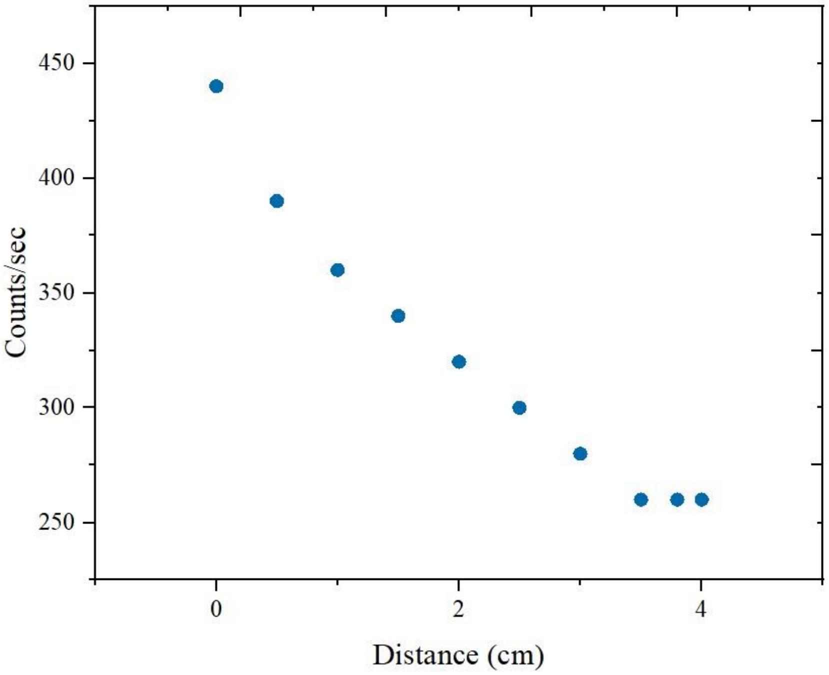

From the table and the plot, it can be observed that the counts per second decreases as the distance increases, until reaching a point where the number of counts is constant. It means that there is no more signal detected. Therefore, the range of alpha particles in air is about ***3.5 cm^{-1}***.

5.1. Range of Alpha Particles in Air by SRIM Simulation (Monte Carlo)

Using the SRIM software, it is possible to observe the simulation of the total path length traveled by alpha particles in the air. Two plots are obtained: the depth vs. y-axis and the ionization (Bragg peak/curve) of the alpha particles. The Bragg curve represents the energy loss rate as a function of the distance through a stopping medium. The Bragg peak is the maximum, and beyond that, the energy deposition drops sharply.

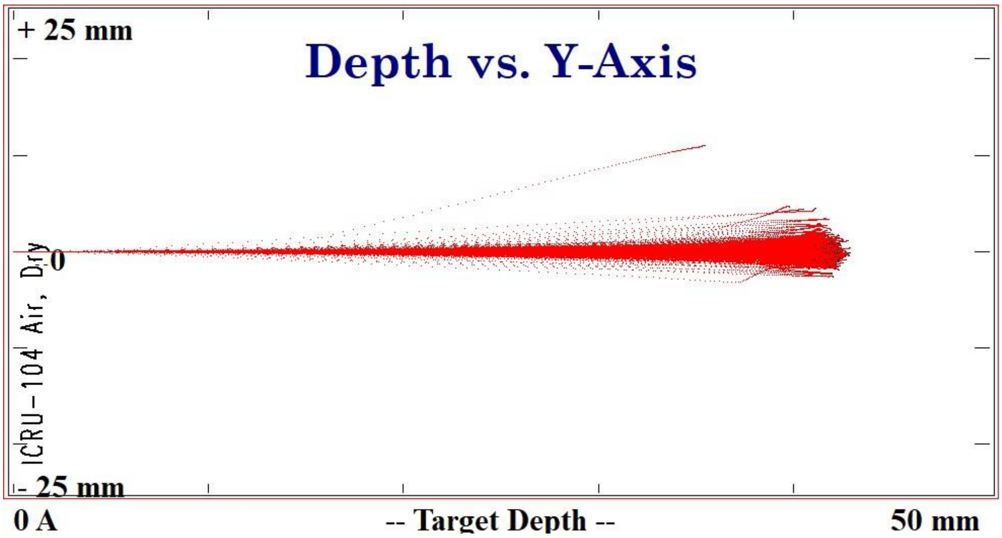

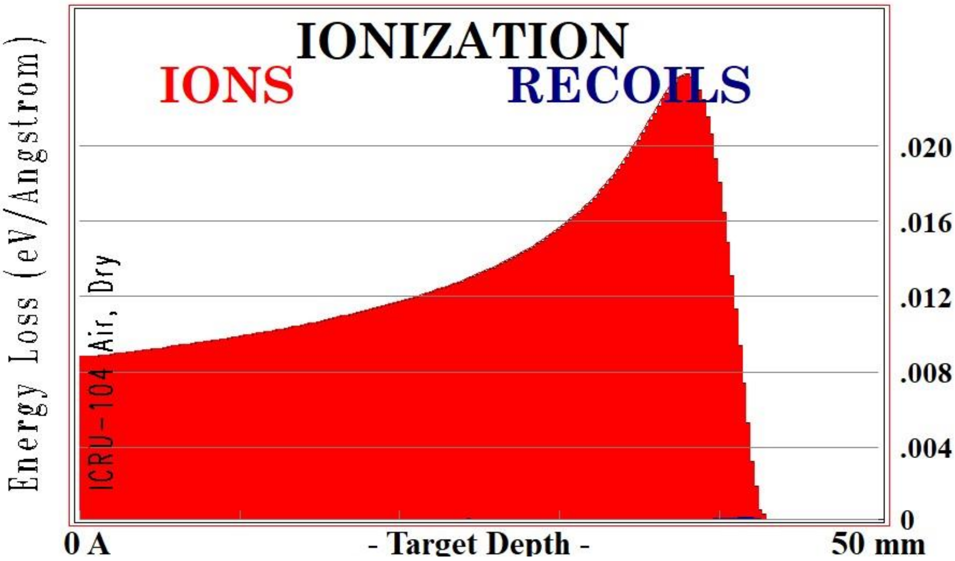

From the two plots, it can be denoted that the intensity of alpha particles decreases when the distance increases. Alpha particles lose their energy when they interact with the particles present in the air. Here, the range of the alpha particles in air is around 3.5 to 4 cm. The Bragg peak is about 4.3 cm and beyond that, the energy decreases sharply until no more signal is detected.

CONCLUSION

In this project, the fundamental components of radiation protection and radiation sources are investigated. This includes the various radiation sources and types, its units and quantification, radiation protection principles, the various scintillation detectors and scintillating crystals, the components of a scintillation detector, peak integration, energy calculation and source identification, attenuation coefficient determination, and range of alpha particles in air. Software such as ROOT, Origin Analysis, Excel, and SRIM simulation are among the programs used the technical specifications of the two scintillation detectors are compared through the experimental methods and outcomes. In contrast to a BGO detector, a NaI detector clearly has a better and more advantageous resolution. But each one has a unique set of characteristics and applications.

The energy of the unknown source is determined from the equation of the calibration line using a known energy. To pinpoint the source, the calculated energy is contrasted with data from the literature. It should be noted that it is only a rough estimate and may not be the source of radiation in its entirety. Due to the possibility of errors during the Gaussian fitting in ROOT, values may vary. The attenuation coefficients of aluminium and copper are determined using the BGO detector at 2000 V and Cs-137 as the radioactive source. The reduction of an x-ray beam as it passes through matter is known as attenuation, and each material has its own attenuation coefficient. This is a critical factor in medical imaging. When the two materials are compared, copper has a higher attenuation coefficient than aluminium. Copper has a higher atomic number and density than aluminium, making it more efficient for shielding. The range of alpha particles in air is determined using the plastic detector, SRIM simulation, and the pixel detector. It ranges from 3 to 4 cm, depending on the detector, the radioactive source, and the intensity of the energy applied. In a nutshell, the project's primary goals have been accomplished.

References

1. Knoll, G. F. (2010). Radiation detection and measurement. John Wiley & Sons.
2. Radiation Detection Scintillators. (2022). Retrieved from Luxium Solutions:
3. Advatech-Radiation Detection/Imaging and Photonics. Retrieved from Advatech UK Limited:
4. Radiation Detection Scintillators. (2022). Retrieved from Luxium Solutions: Schauer, D. A., & Linton, O. W. (2009). NCRP report No. 160, ionizing radiation exposure of the population of the United States, medical exposure—are we doing less with more, and is there a role for health physicists?. Health physics, 97(1), 1-5.

5. United Nations Scientific Committee on the Effects of Atomic Radiation. (2017). Sources, effects and risks of ionizing radiation, united nations scientific committee on the effects of atomic radiation (UNSCEAR) 2016 report: report to the general assembly, with scientific annexes. United Nations.
6. Radiation Doses. (2020, December 22). Retrieved from Canadian Nuclear Safety Commission:
7. Valentin, J. (2007). The 2007 recommendations of the international commission on radiological protection (Vol. 37, No. 2-4, pp. 1-133). Oxford: Elsevier.
8. Cember, H., Introduction to Health Physics, 3rd Edition, McGraw-Hill, New York (2000).
9. Attix, F.H., Introduction to Radiological Physics and Radiation Dosimetry, Wiley, New York (1986).
10. Martin J.E., Physics for Radiation Protection, Wiley-VCH Verlag Gmbh